

NIR Single Pixel Camera

By:

J. Ryan Stinnett
Jennifer Gillenwater

NIR Single Pixel Camera

By:

J. Ryan Stinnett
Jennifer Gillenwater

Online:

< <http://cnx.org/content/col10525/1.1/> >

CONNECTIONS

Rice University, Houston, Texas

This selection and arrangement of content as a collection is copyrighted by J. Ryan Stinnett, Jennifer Gillenwater.
It is licensed under the Creative Commons Attribution 2.0 license (<http://creativecommons.org/licenses/by/2.0/>).
Collection structure revised: April 29, 2008
PDF generated: February 4, 2011
For copyright and attribution information for the modules contained in this collection, see p. 34.

Table of Contents

1 Project Introduction	1
2 Compressive Imaging	7
3 Projector Setup and Issues	11
4 DMD Development Kit Setup and Issues	19
5 Project Summary	25
Bibliography	30
Index	33
Attributions	34

Chapter 1

Project Introduction¹

1.1 Problem Statement

The ability to image sketches hidden by layers of paint is a valuable asset to art purchasers in their attempts to exhaustively examine the works they collect. Art conservators value a painting's underdrawings for two main reasons. The first is that underdrawings can be exploited as an aid in determining whether the painting is an original or a forgery, by comparing the style of the underdrawings to those of an artist's other works. The second is that comparisons between a painting and its own underdrawing can give new insights into an artist's creative process for that work of art. Underdrawing images are best revealed by near infrared (NIR) cameras because all paint pigments, except black, are somewhat transparent in the 900 - 1700 nm range[24]. However, current NIR cameras that are sensitive in this wavelength range are exorbitantly expensive, typically costing around \$50,000[22]. This leaves the market of small art museums and individual art collectors unaddressed. We intend to deliver an NIR camera that meets or exceeds key imaging system parameters in this market, such as spectral range, image resolution, capture time, and portability, while also reducing cost below the \$5,000 level.

1.2 Background

Before the 1960s, there was only one way to examine a painting's underdrawing: the layers of paint in front of the underdrawing had to be removed, thereby destroying the painting in the process. This was unacceptable for multiple reasons. Since underdrawings are typically of less interest than the finished painting, removing the layers of paint on top is not justified. Also, many interesting results come from a detailed comparison between the original painting and its underdrawing. This comparison is difficult if the paint layers must be destroyed to access the underdrawing.

J. R. J. van Asperen de Boer was the first to image underdrawings using NIR reflectography in 1968 [26]. Previous attempts had used an NIR camera to passively capture light in that range. However, with passive capture it was difficult to see through pigments such as green, since most of the light collected was in the range of 750 - 900 nm, which is below the range where those colors are transparent. Boer solved this problem by capturing the reflected light from a tungsten lamp that produced radiation of wavelengths up to 2500 nm, giving a much clearer image of the underdrawing. While Boer's design has been improved in numerous ways during the past four decades, it remains fundamental to most techniques for imaging underdrawings nondestructively.

Figure 1.1 and Figure 1.2 below are examples of comparisons between original paintings and their underdrawings as captured with a typical modern NIR camera. In Figure 1.1, the underdrawing shows that the man in the top hat, the artist's accountant, was initially looking towards the viewer, but later this changed

¹This content is available online at <<http://cnx.org/content/m16124/1.1/>>.

so that he looked away, purportedly because of disagreements between the two men [8]. In Figure 1.2, a large arrow can be seen on the chest of a horse on the underdrawing of a painting by Laib. This arrow is absent from the overlaid painted image.



Figure 1.1: Comparison between NIR and visible range images of a Renoir painting [8].

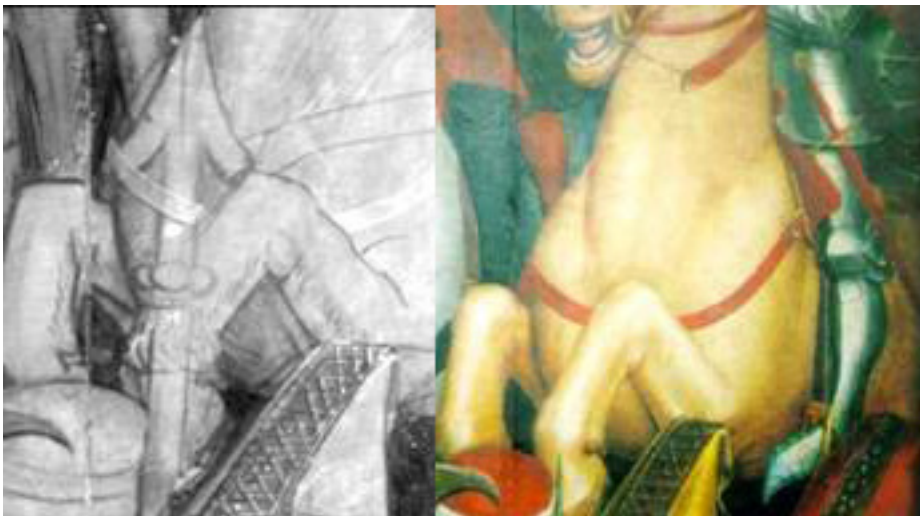


Figure 1.2: Comparison between NIR and visible range images of a Laib painting [9].

Unfortunately, conventional NIR cameras that cover the spectral range required for a clear image of un-

derdrawings typically cost from \$30,000 to \$50,000. By reducing the cost of the NIR camera, underdrawings could be examined by a much larger set of universities, museums, and collectors. This opens numerous opportunities to gain deeper insight into both the creative process and the history of artwork.

1.3 Problem Requirements and Specifications

The spectral range of a camera depends on the type of detectors it employs. Thus, whatever the overall structure of our design, it will have to incorporate a sensor capable of imaging through paint. All pigments except black are somewhat transparent in the 900 - 1700 nm range, which can easily be covered by any NIR detector [24]. Even though our problem probably constrains us to using an NIR detector of some sort, this still leaves us a variety of options. We will want to choose a detector that has minimal cost, in order to keep the final camera price low. We will also want a detector that is appropriately sized so that it can easily be physically integrated into our overall optical system. Additionally, we will need to ensure that any detector we choose is capable of providing the dynamic range required for underdrawing imaging. That is, 256 grey levels should be distinguishable in the image [14].

As Boer found in his original experiments with reflectography, for high-quality underimaging a specialized light source is necessary, to provide coverage of all relevant wavelengths in the NIR range [26]. Our system would also need such a source of radiation. For this source, or sources, 800 W of power is a high enough value to give a good signal-to-noise ratio (SNR) in standard room temperature conditions [20]. Using significantly higher power is not advisable, as most sources will emit a certain portion of their light in the UV and visible ranges, and it will be difficult to filter out all of this. Intense light from these high-energy ranges could damage a painting during imaging.

The image acquisition time when imaging underdrawings is quite flexible. While experience with conventional charge-coupled device (CCD) or complementary metal-oxide-semiconductor (CMOS) digital camera technology in the visible range would lead one to expect image acquisition time on the order of μsec , such a short acquisition time is not critical for this application. A relatively small number of images are typically taken with a static target. The resulting images are typically subjected to extensive analysis and comparison with similar images of underdrawings from the same artist. When all of these factors are taken together, a small image acquisition time becomes a nice extra feature when possible, but is not crucial for success in this application domain. Typical systems targeted towards underdrawing imaging take about 15 minutes to acquire and process an image due to the mosaicing system used. For the underdrawing imaging application, the relaxed image acquisition time requirement makes it possible to consider sacrificing low acquisition time for improved image quality, improved image resolution, or reduced camera cost.

Portability is a valuable and highly preferred feature for underdrawing inspection. For cumbersome systems, or systems that are difficult to relocate, artwork can be moved to the location of the camera for inspection. However, this need for transportation puts the original artwork at risk for damage. Since such great care is needed to move the artwork, a portable camera would be a much better solution since it removes this potential hazard. Reducing the risk of damage to the original artwork is critical because, while it is generally possible to replace a broken camera, it is impossible to replace the artwork.

While analyzing underdrawings does not directly mandate a specific image resolution, one must be able to make out the various lines with reasonable clarity in order to derive meaningful results. By image resolution, we mean a pixels / mm specification for the final reconstructed image of the underdrawing. A camera with a low image resolution could be used, but one would need to take many pictures by zooming in on small parts of the target. These pieces would later need to be aligned and stitched together to view the entire underdrawing, a process which is time consuming and could be quite involved for the user. A better approach is to use a camera with a larger image resolution which can capture the entire underdrawing or areas of interest with only one or several pictures. According to our initial research, a system that can provide at least 2 pixels for each mm of target length should be sufficient [25]. We expect to use our design with small to medium paintings, as indicated by the average target size of 0.33 m x 0.33 m. This assumes our system will have a field of view (angular observable range) comparable with the largest artwork size.

1.4 Existing Technologies

There are a variety of systems that can be used to image underdrawings. Most contain as their central component cameras such as the two listed in the table below.

Five alternatives for the detector component of such cameras were surveyed by Gargano, Ludwig, and Poldi in their recent comparison of IR reflectographic systems [20]. They analyzed CCD Si, FPA InGaAs, FPA HgCdTe, InSb detectors, and vidicon tubes. The respective upper spectral limits for these sensors are 1050 nm, 1700 nm, 2500 nm, 5 nm, and 2 nm. Using pigments modeled after those used in the 15-16th centuries, they measured the pigment transparency that could be achieved with each sensor.

Their conclusion is that InGaAs sensors are best, as they achieved high transparency values and exhibited a large gray range. However, this result only holds for underdrawings made with black, carbon-based drawing implements; since black pigments have only 2% transmittance in the NIR range, they will not be transparent for any of the five devices analyzed. For underdrawings made with iron gall inks, red crayons, or grayish inks, CCD Si cameras are probably best, since these substances are usually completely transparent over 1200 nm. Our project would focus on providing better imaging for black underdrawings only, since, for imaging other types, the best system, CCD Si, is already relatively low-cost.

Current underdrawing imaging systems that use sensors other than the cheap CCD Si require image scanning to achieve adequate image resolution. This is because their sensor arrays are small, on the order of 320 x 256 pixels; it is not economically feasible to build larger arrays. Over the past decades, scanning systems have made advances in precision of motion control and image assembly [16]. However, in the image reconstruction process, they still face difficulties with perfecting image mosaicing.

The best systems to date resemble the CPS 200E positioning system, which moves the camera while the painting stays stationary [10]. This is advantageous from an art conservation standpoint, in that it reduces wear on the painting. The CPS 200E device achieves very accurate motion. However, accurate motion alone is not enough to ensure high image quality. The complexity of the image mosaicing task also requires very precise control of lighting and knowledge about the geometric distortion produced by the exact positioning of the camera in the scanning frame. Lighting control can be achieved by imaging an illumination control card to detect inhomogeneity. Geometric distortion can be measured by imaging graph paper. The information from these two images is then merged with that of the other images during the mosaicing process.



Figure 1.3: CPS 200E scanner at work [10].

Aside from the camera and positioning system, the lighting mechanism is the most important element in modern underdrawing imaging systems. To reduce any damage to a painting, high-energy light, such as that from the visible and UV ranges, should be filtered out during imaging. However, the intensity of the light source must be high, since this value greatly influences the SNR of the detector. In one typical imaging setup, a pair of halogen bulbs, each with intensity in the 400 W is used [17]. The light from these bulbs is passed through an RG 1000 filter and a BG 39 filter, which sufficiently reduces high-energy radiation without damaging IR imaging potential.

The existing solutions to the various aspects of the underdrawing imaging problem - NIR detector, camera-painting positioning system, mosaicing techniques, and illumination schemes - are inadequate. They combine to make systems which, while cheaper than using a single huge NIR sensor array to take a single image, derive their economical advantage partly at the expense of system portability, accuracy, and simplicity. We intend to implement a different alternative to the single huge NIR array. Our alternative would improve upon the current solutions by reducing overall system cost, perhaps not only in monetary terms, but also in terms of portability, accuracy, or simplicity. What current systems offer for \$50,000, we intend to match or beat for under \$5,000 [22].

Chapter 2

Compressive Imaging¹

In order to achieve the goals set out in the project introduction, we intend to exploit compressive sensing. The reasoning behind our choice of this technique and the technique itself are described in detail in the following paragraphs.

A conventional digital camera works by capturing light from an object and focusing it through a lens onto an array of sensors. Cameras used by the general public operate in the visible range, 400 to 750 nm, with CMOS sensors. They can be modified to image in a slightly wider range, from 280 to 1200 nm, if their infrared (IR) filters are removed [1].

Current IR cameras can operate in much higher ranges, from the near infrared (NIR) at 0.75 – 1.4 μm , to the far infrared (FIR) at 15 – 1,000 μm [2]. The average person, however, does not have the purchasing power to buy an IR camera, as one generally costs between \$3,000 and \$50,000[23]. Even for companies or governmental institutions, this is a substantial sum of money.

The bulk of the cost of an IR camera is in its sensor array and the cooling system that regulates the array's temperature. The array alone accounts for at least one-third of any IR camera's price. The cooling system that helps reduce background noise and the effects of pixel bleeding is similarly expensive. Unfortunately, there is no Moore's law for these sort of components. Unlike transistors, IR sensors and their cooling systems are not likely to decrease in size or cost anytime in the near future. Thus, while the camera's image processing chips will probably become cheaper in the next few years, no such reduction in cost can be predicted for the sensor components. In fact, as the general trend in the camera industry is toward more pixels, it is likely that soon the cost of an IR camera will be almost solely determined by the price of its sensor array and this array's cooling system.

Therefore, to create an economical IR camera, the number of sensors and cost of their cooling system would have to be dramatically reduced, without severely damaging the camera's resolution. The technology to do this already exists; it is called compressive sensing. In principle, a compressive sensing device needs only a single sensor—a single pixel. Not only does the use of a single pixel remove the price of a sensor array from the picture, but also it has the potential to reduce the cost of the sensor cooling system. Since a single pixel device does not suffer from the pixel-bleeding problem that necessitates a high-quality cooling system in regular IR cameras, in a single-pixel camera an inexpensive cooling alternative just for removing background noise could be used.

2.1 Compressive Sensing Hardware

The basic operation of a compressive sensing camera is relatively simple. Light from an object is focused by a lens onto a digital micromirror device (DMD). A DMD is an array of tiny mirrors that can be tilted $\pm 10\text{-}12^\circ$, from “on” to “off” positions [3]. In the “on” state, these mirrors reflect light from the object to a secondary lens, which focuses this light to the sensor. Data from this sensor is sent to a signal processing unit, which

¹This content is available online at <<http://cnx.org/content/m16125/1.1/>>.

manipulates data points to construct an image of the original object. To generate a set of useful data points for image reconstruction, the mirrors of the DMD are flipped into a series of random configurations, in each of which approximately half of the mirrors are in their on position.

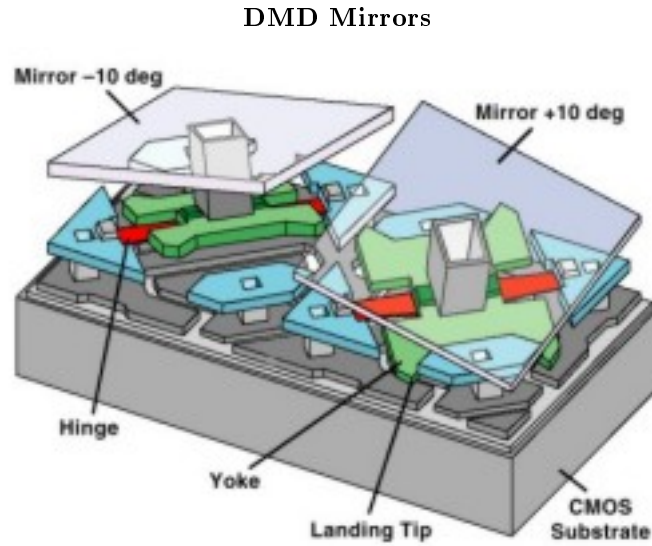


Figure 2.1: Close-up diagram of two typical DMD mirrors [4]

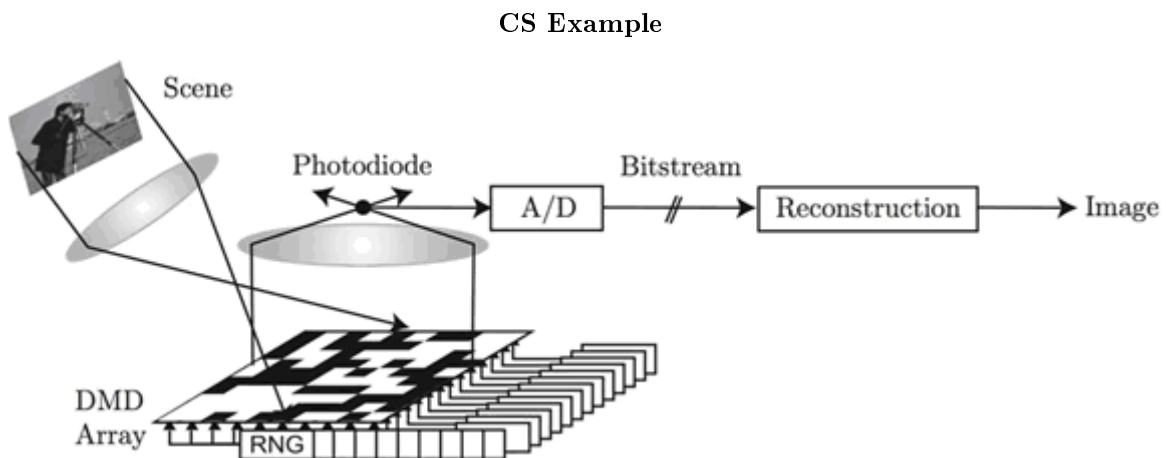


Figure 2.2: How a compressive sensing camera works [13]

2.2 Standard Imaging Theory

For an N -pixel image, N samples are taken. Then, since this is usually too many samples to store or transmit, the data is compressed. Transform coding is used to perform the compression. This takes a sample vector x and expresses it in basis Ψ , as shown in the figure below. Then, x can be specified just by the K -sparse matrix s , which has K much less than N non-zero values. One example of a typical Ψ matrix is the discrete cosine transform (DCT) used for JPEG. This works well for natural images, as they tend to be sparse in the DCT.

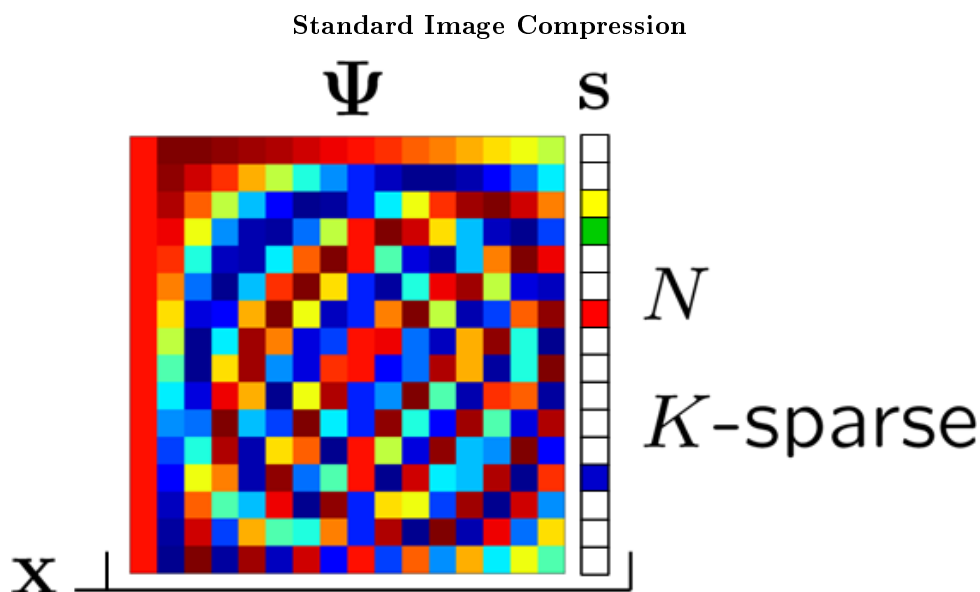


Figure 2.3: $x = \Psi s$ [13]

The standard approach is lossy. $N - K$ samples are thrown away, and only the K values from s are stored or transmitted. This means that removed data cannot be recovered afterwards, so the quality of the image cannot be improved later.

2.3 Compressive Sensing Theory

The standard sample-then-compress process can be simplified. Consider directly acquiring a signal in a compressed representation. Say we obtain M less than N measurements and place them in the vector y . Then y is equivalent to the inner product of x and M other vectors (where x is the N -sample vector from the standard sampling example). If we stack these M other vectors into the matrix Φ , then the overall equation becomes $y = \Phi x = \Phi \Psi s$. This is illustrated in the figure below.

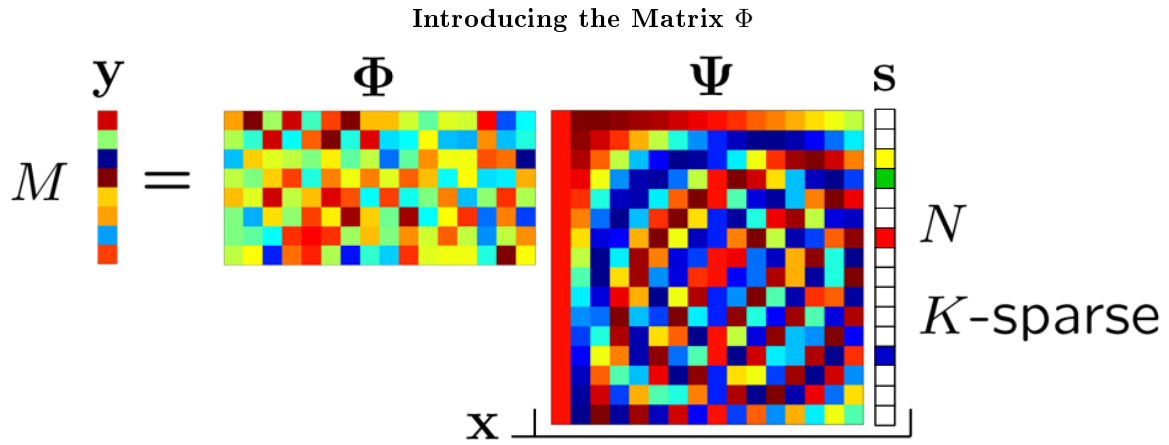


Figure 2.4: $y = \Phi x = \Phi \Psi s$ [13]

Gaussian noise actually works quite well for creating the Φ matrix. So, the only really difficult math to be done here is in designing a reconstruction algorithm to obtain x from y . This is a complex process, but faster methods are developing rapidly.

Chapter 3

Projector Setup and Issues¹

To implement a compressive sensing camera, the most vital element is the DMD. There are two practical alternatives for incorporating a DMD into a prototype:

- Use the DMD that is built into a standard DLP projector, or
- Buy a TI Discovery Board kit.

We chose to investigate the projector option first, as it offers a compact structure with a lamp and set of lenses already built in. The following paragraphs and images walk through the work we did to attempt to adapt the projector into an NIR camera.

The overall system we worked with consisted of the projector and the surrounding components that can be seen in the figure below. The basic flow of control in this system is as follows:

1. Laptop sends random frames to the projector
2. Projector light, modulated by the frames on the DMD, is projected on to the target object
3. Light reflects off the target back towards the projector
4. Zoom lens beside the projector captures the reflected light and focuses it down onto a photodiode
5. Photodiode output goes through a preamplifier and filter
6. Filter output feeds into a DAQ
7. DAQ output is sent back to the laptop for reconstruction into the target image

¹This content is available online at <http://cnx.org/content/m16126/1.1/>.

Overall System

Figure 3.1: Laptop, projector, zoom lens, and DAQ

The image below shows the zoom lens that we used to focus reflected light onto our photodiode. This photodiode has both an NIR detector and a visible detector. Both have a 1.5mm diameter active area, onto which the zoom lens needs to focus all the light it takes in. We had great difficulty getting this focus correct. Ultimately, we ended up focusing it by connecting the output of the photodiode to an oscilloscope, then turning the fine and coarse focus knobs until the maximum signal was achieved. Even with careful focusing, we only obtained max measurements of about 100mV for the NIR signal, when all mirrors of the DMD were turned to their "on" position.

Zoom Lens



Figure 3.2: 10x zoom lens with photodiode mounted at focal point

To combat the zoom lens focusing difficulties and try to achieve a greater signal at the photodiode, we investigated different lamp alternatives. The standard projector lamp we originally worked with, pictured below, has a power of 200W. Much of its output is not in the NIR range, however. Thus, we found a 100W bulb with its peak emittance at 1 micron, and ordered it. However, replacing the projector bulb with this new bulb proved very cumbersome. The new bulb required a different power supply (12V, 8A, DC) than the projector bulb, so we had to buy a separate power source for it. Additionally, the projector has a safety feature which requires that something be attached to its lamp socket, or else it will not run. So, we had to make a set of connectors for the original projector lamp so that we could remove the lamp from its place inside the projector. After all of this, though, in the end we found it prohibitively difficult to mount the new bulb in the projector, as we could find no good way to secure it in place.

Projector Lamp

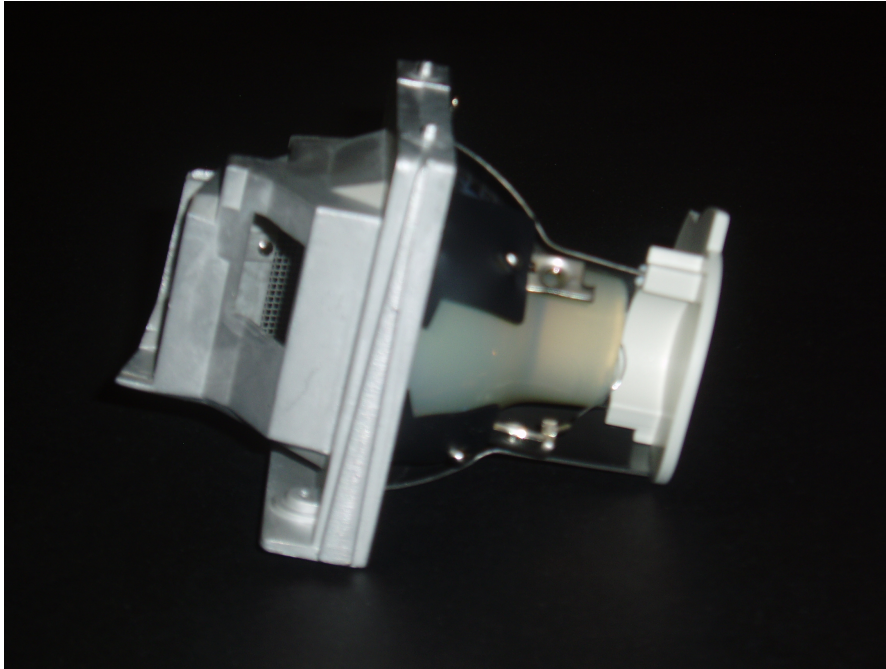


Figure 3.3: Standard mercury lamp from an Optoma projector

In addition to difficulties with the light source and focusing lens, we also had trouble with speeding up image acquisition time. We originally were sending frames to the projector from a standard MATLAB script. This was very slow. Using the Psychtoolbox plugin allowed us to take advantage of frame buffering [12]. This sped up the rate to between 15 and 50 frames per second (fps). The frames shown in the video below change at a rate in this range.

Random Frames

This is an unsupported media type. To view, please see <http://cnx.org/content/m16126/latest/movie.mpg>

Figure 3.4: Illustration of random frames displayed as MATLAB movie

To further decrease capture time we tried exploring tighter control of the projector's image display capabilities. Although the video frame rate is 60 Hz, which is the maximum rate at which the projector can receive images, the mirrors on the projector's digital micromirror array (DMD) flip at a rate of at least 1000 Hz. Possibly, the mirror flip rate may even be as fast as 9800 Hz [21]. So, we wanted to use every

mirror flip as a random frame for our CS measurements, rather than just using each video frame to take one measurement. The result would be such that for each video frame, we would obtain between 16 and 164 measurements. Ultimately, if for a 1-megapixel image we required 100,000 frames, then this could give an image capture time of 10 to 50 seconds.

In order to exploit each individual mirror flip, we needed to understand pulse width modulation (PWM). This is the scheme that the projector uses to determine mirror flipping. Under normal operation conditions, PWM is used to simulate grayscale values of image frames. For example, consider the image in the figure below. In this image, the grayscale of the right half is true while the grayscale of the left half is an illusion: the left half in fact contains only black and white dots, no grey. A projector creates the grayscale illusion in a similar manner. By rapidly toggling its mirrors between "on" to "off" positions, it tricks the eye into perceiving a series of black and white squares as grey. The "on"/"off" pattern is determined according to PWM.

Grayscale Image



Figure 3.5: Mirror flickering on a DMD creates the illusion of grayscale through PWM [11]

Our investigation of PWM schemes led us to understand that basic PWM works as illustrated in the example of the figure below. First, the time allotted for a video frame (1/60th of a second) is divided into blocks. There is one block for each bit of a pixel's grayscale value. If grayscale values can range between 0 and 31, then 6 blocks are created. For the length of each block, the mirror will either be turned to its "on" position if the bit associated with the block is a 1, or its "off" position if the bit associated with the block

is a 0. This is an acceptable method for creating a grayscale effect using only black and white projections. However, the long duration of blocks associated with higher-order bits can produce effects that are jarring to the eye.

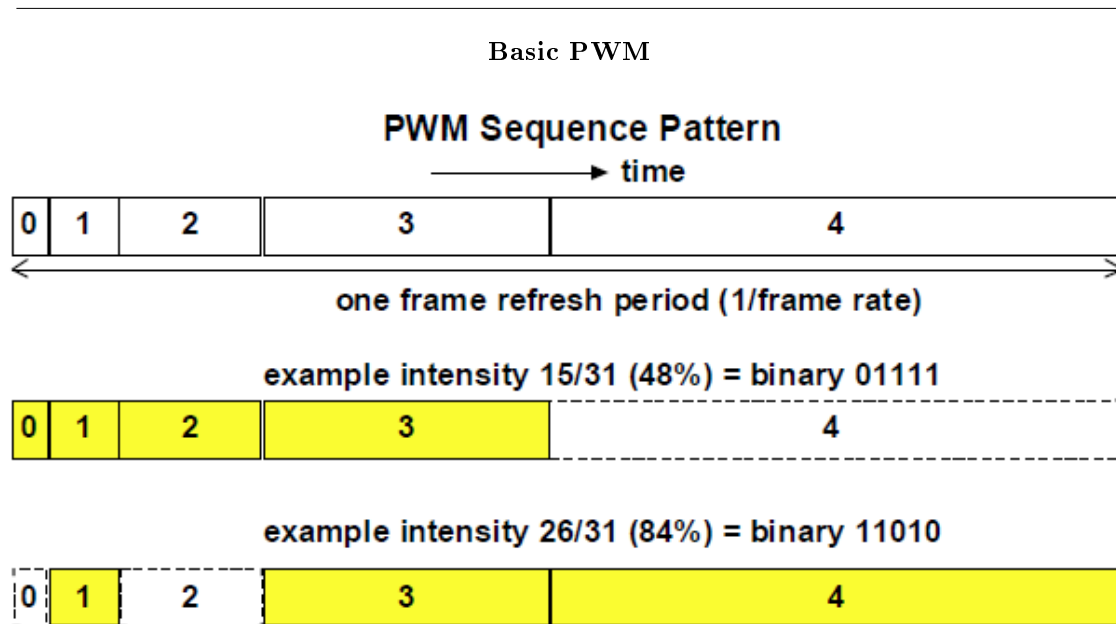


Figure 3.6: An example of how basic PWM works [18]

A smoother version of PWM is used in most projectors, to reduce the jarring effects seen with basic PWM [18]. The methodology of smooth PWM is illustrated in the example below. This modulation scheme devotes the same amount of time to each bit as basic PWM. However, instead of laying the blocks for each bit end-to-end, it breaks them up into smaller packets and mixes them up. Each block from basic PWM becomes a series of blocks in smooth PWM. These smaller blocks are spread out over the entire time for a frame, alternating with blocks that represent the other bits of the desired grayscale value.

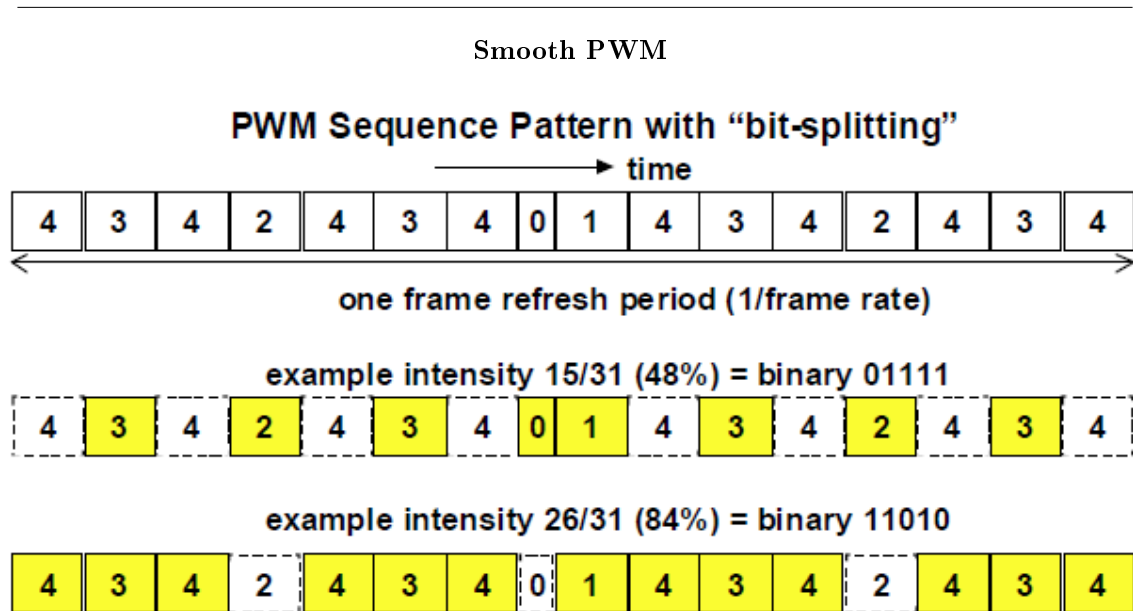


Figure 3.7: An example of how smooth PWM works [18]

After completing textbook research of PWM, we attempted to observe PWM patterns in the lab. We sent the projector frames with known grayscale values and captured the mirror-flipping with a visible-range photodiode. However, the mirror-flipping patterns we observed with this approach did not resemble anything like what we had expected. They looked something like the plot shown in the figure below. At first we thought the problem must be on the photodiode end. Yet, the specification sheet for the photodiode listed its response time in the nanosecond range. So, we took another look at the documentation of PWM available on TI's website, and emailed some TI representatives to see if they could give us some insight on the problem. From these sources, we learned that the PWM scheme employed by current DLP projectors is very much more complex than that described in the examples of basic and smooth PWM above. Although smooth PWM may be a part of what current projectors use, the actual mirror flipping patterns are determined based on an algorithm that takes into account a large variety of projector settings. We were told that, in fact, TI considers their mirror-flipping algorithms proprietary, as these codes contribute to the projector's image quality.

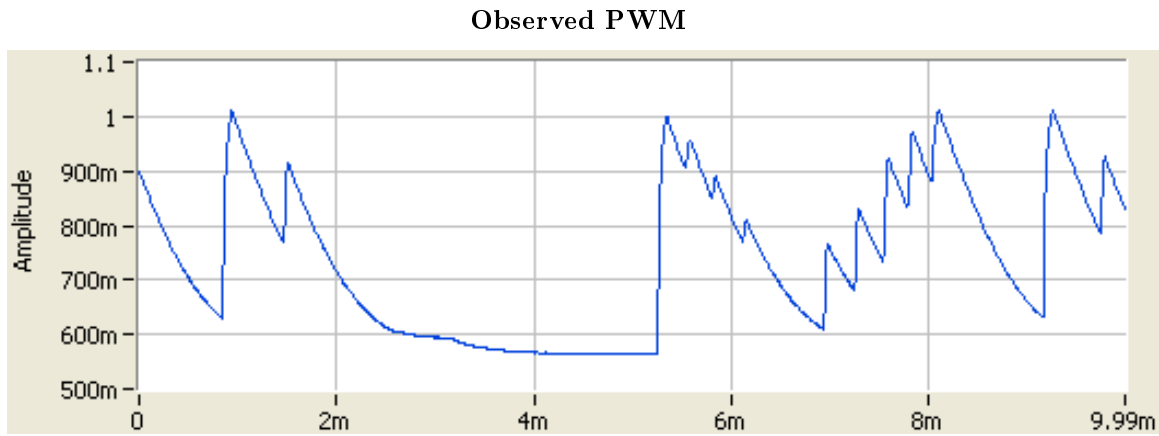


Figure 3.8: Mirror flipping for the grayscale value 67

Due to the multitude of dead ends we ran into trying to create a projector-based version of a compressive sensing NIR camera, we turned to working with a stand-alone DMD board for the last few months of our project.

Chapter 4

DMD Development Kit Setup and Issues¹

After running into many dead ends trying to create a projector-based compressive imaging NIR camera, we did some work with a stand-alone TI board, in a lab table setup. Before we began working on this project, a similar setup already existed, as shown in Figure 4.1 (Original Lab-table Setup). Our lab table setup is very similar, with the exception that we have black cardboard barriers to shield the photodiode from the light source. Our photodiode, light source, and target object are also of course different from those shown in Figure 4.1 (Original Lab-table Setup). Figure 4.2 (Camera Front End), Figure 4.3 (Camera Top View), and Figure 4.4 (Camera Back End) show what the new setup looks like.

¹This content is available online at <http://cnx.org/content/m16127/1.1/>.

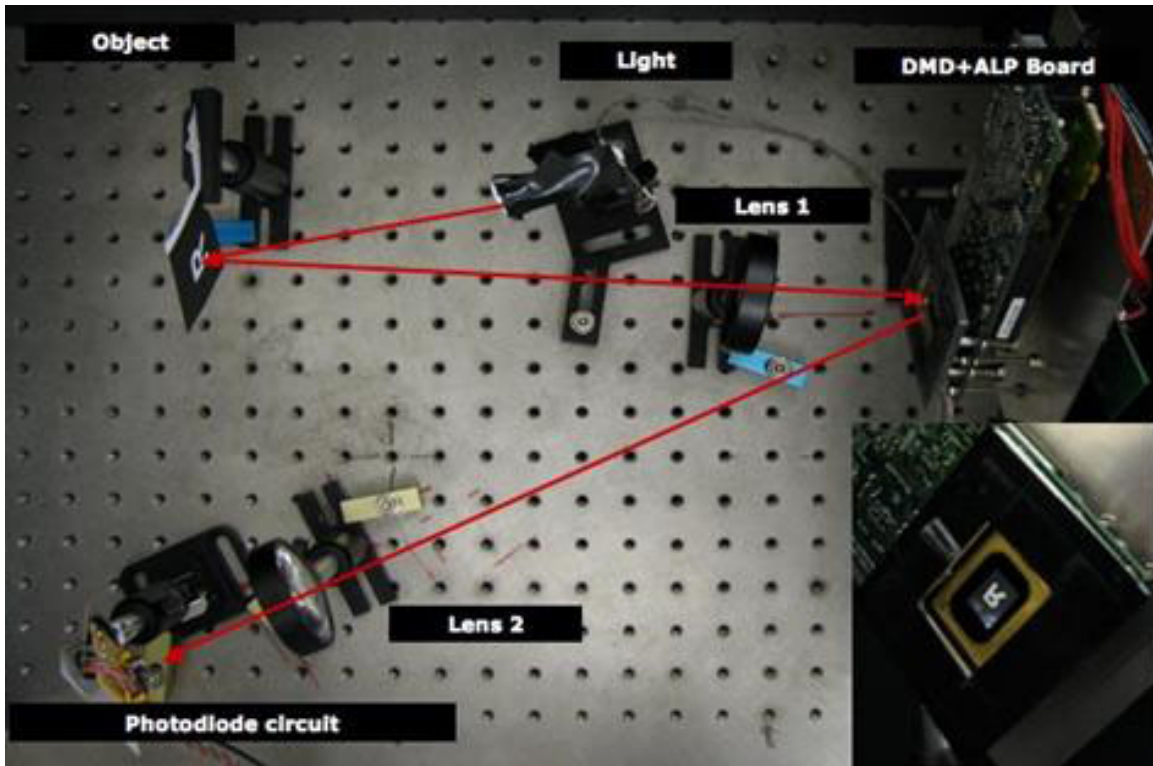
Original Lab-table Setup

Figure 4.1: Original lab-table version of a compressive sensing camera [5].

Camera Front End

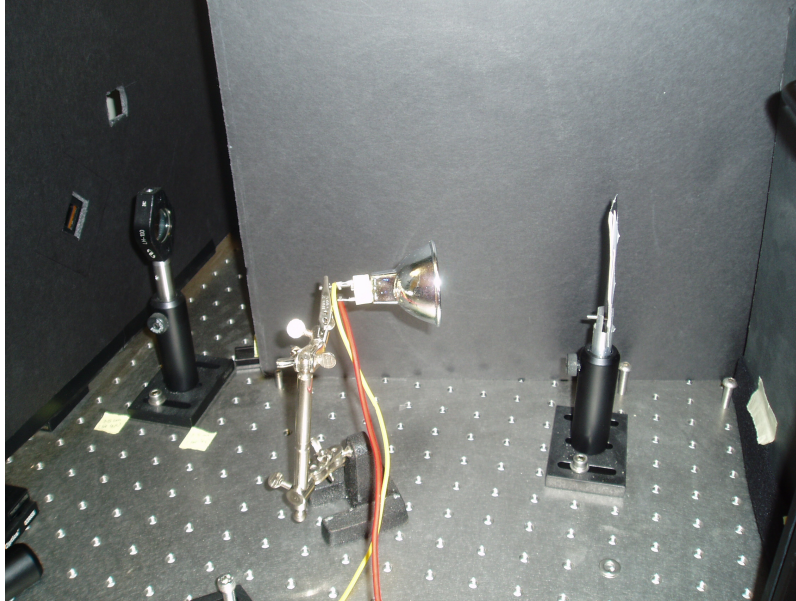


Figure 4.2: Light source, target object, focusing lens, and DMD

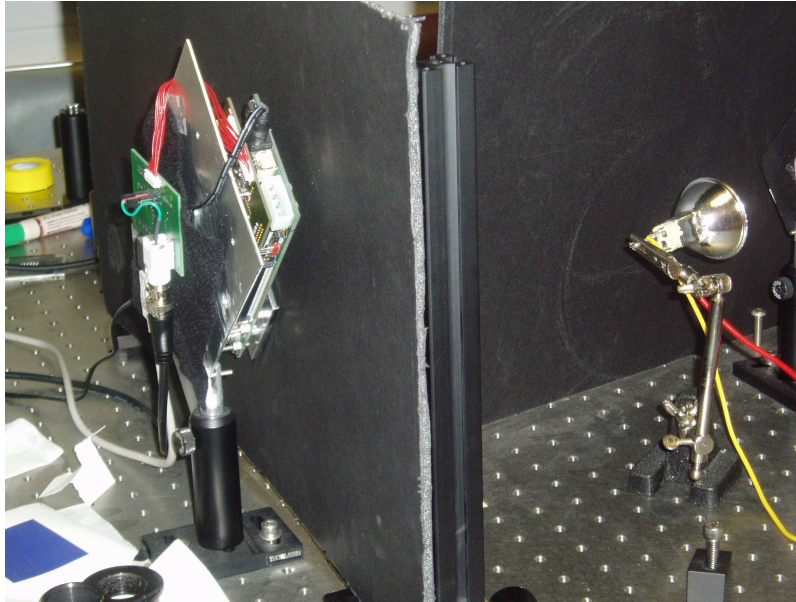
Camera Top View

Figure 4.3: TI 1100 Discovery Board and light source

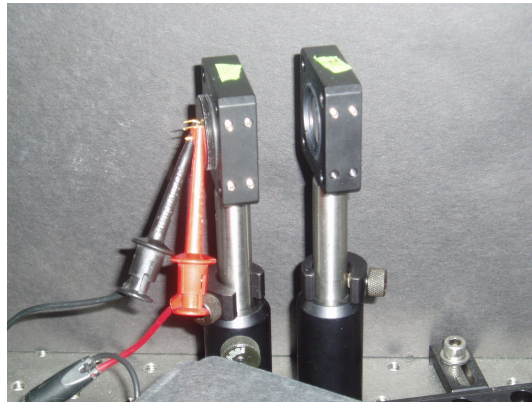
Camera Back End

Figure 4.4: Focusing lenses and photodiode

With this setup, we have direct control of the DMD mirrors; the TI 1100 Discovery Board has a high-speed interface that we can control using ALP (Application Programming Interface) software. To capture diode data, we use VILogger, then clean up the resulting stream in MATLAB. Thus, it seems probable that

with such a setup, achieving a fast capture speed is within reach.

However, we continued to experience problems on the NIR lighting and sensing ends of the camera. The light bulb burnt most substances we tried to mount it on, and had to be positioned just right in order to reflect enough light off the target object. Further, the diode data showed a lot of noise when the signal was low, as can be seen in Figure 4.5 (Noisy Diode Data). Over a long capture period, we also often observed a drift in the base signal, as shown in Figure 4.6 (Drifting Diode Baseline).

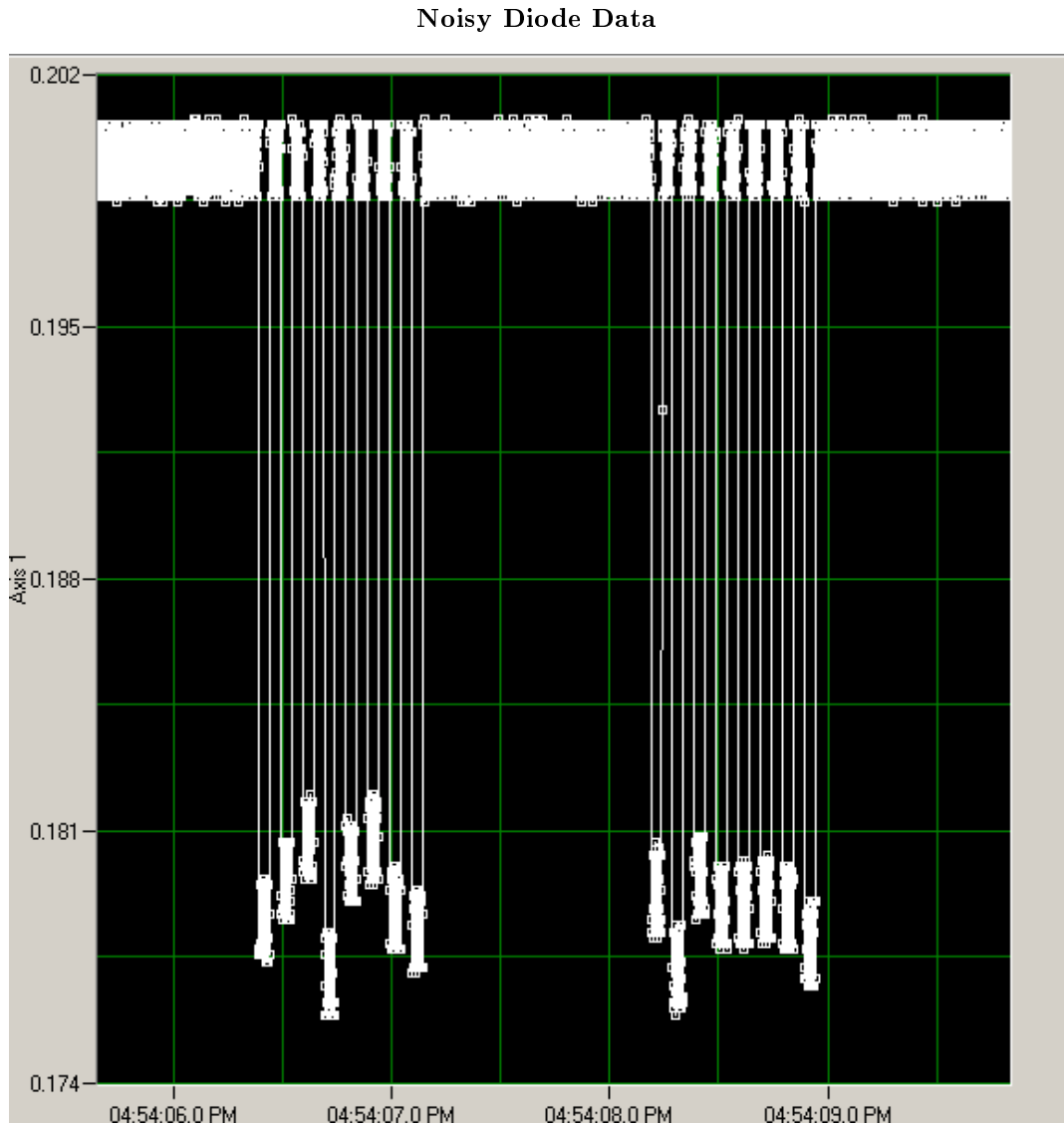


Figure 4.5: Each set of pulses should be flat, as each is a set of the same random frame sent out repeatedly; the diode signal is clearly noisy

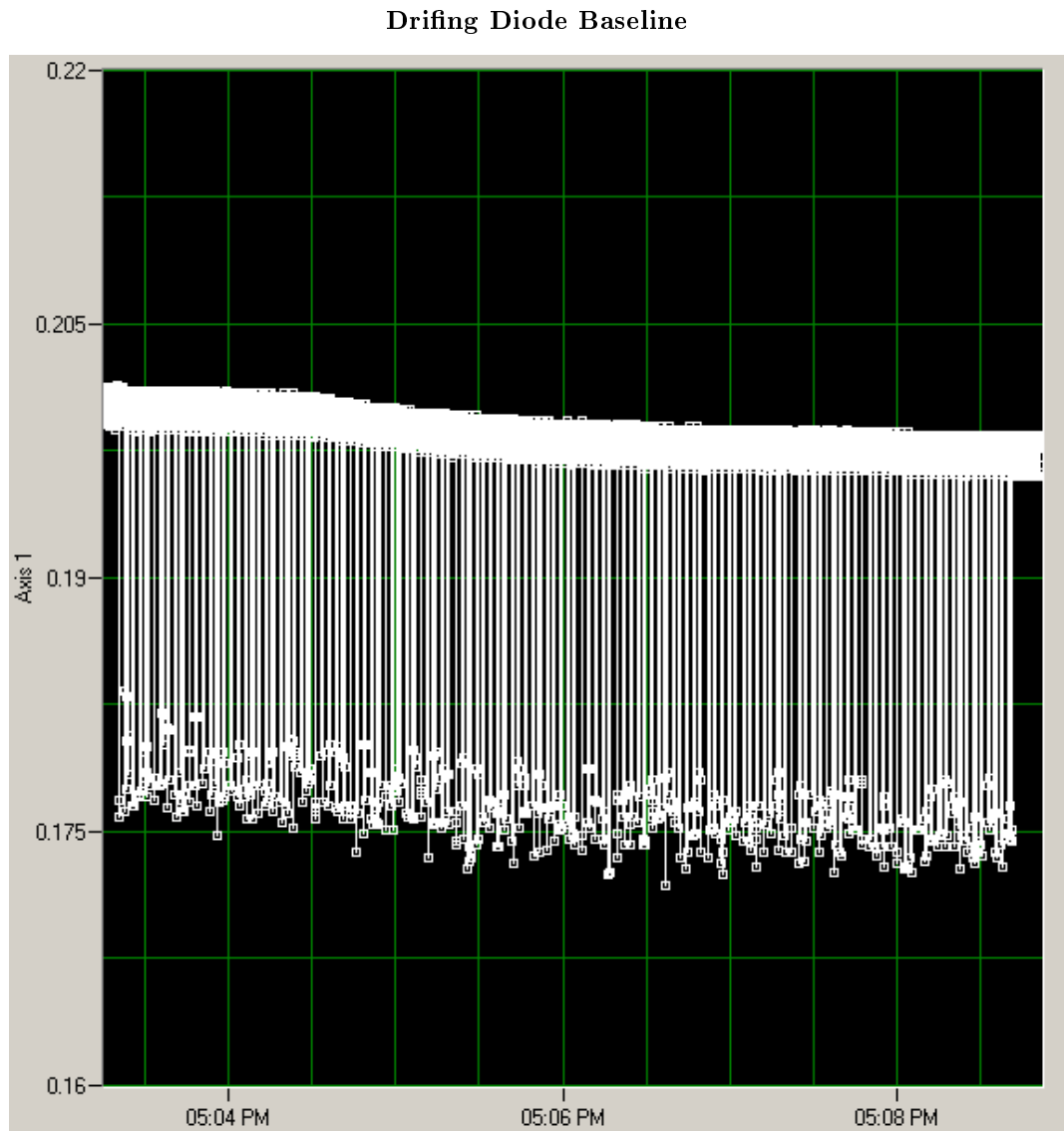


Figure 4.6: Over a capture period of several minutes, the base diode signal decreases significantly

Chapter 5

Project Summary¹

With the projector camera, we attempted to image many different targets. These ranged from fruit to sheets of metal. The clearest images we took were of a "K" cut out of a sheet of metal. These images were our best because metal is a good reflector of NIR light, which meant we had a strong signal at the photodiode. Both a visible and an NIR image of this K are shown below.

¹This content is available online at <<http://cnx.org/content/m16128/1.1/>>.

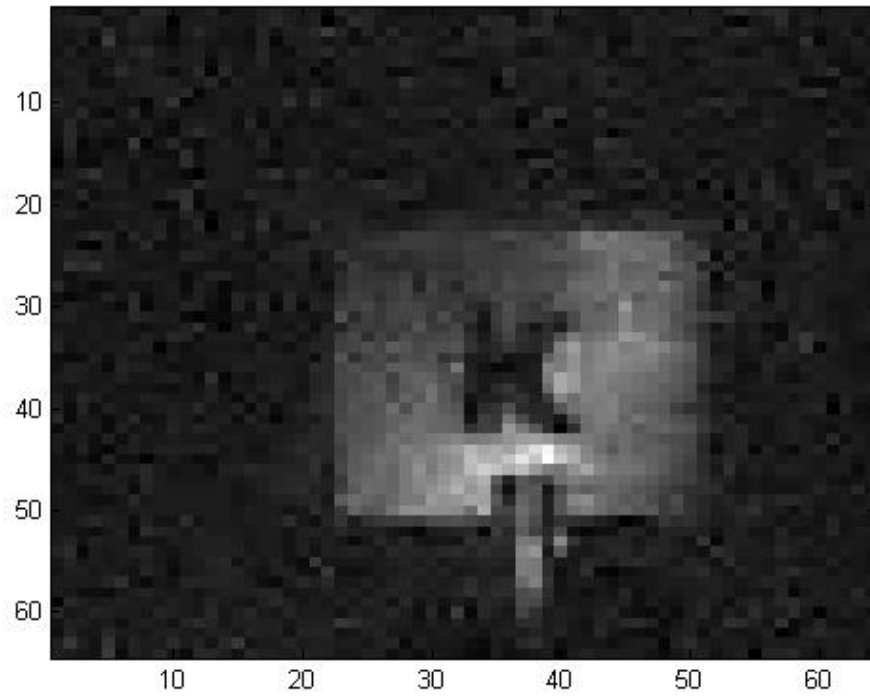
Visible Image of a K

Figure 5.1: 64x64 image, taken using 1600 Walsh patterns

NIR Image of a K

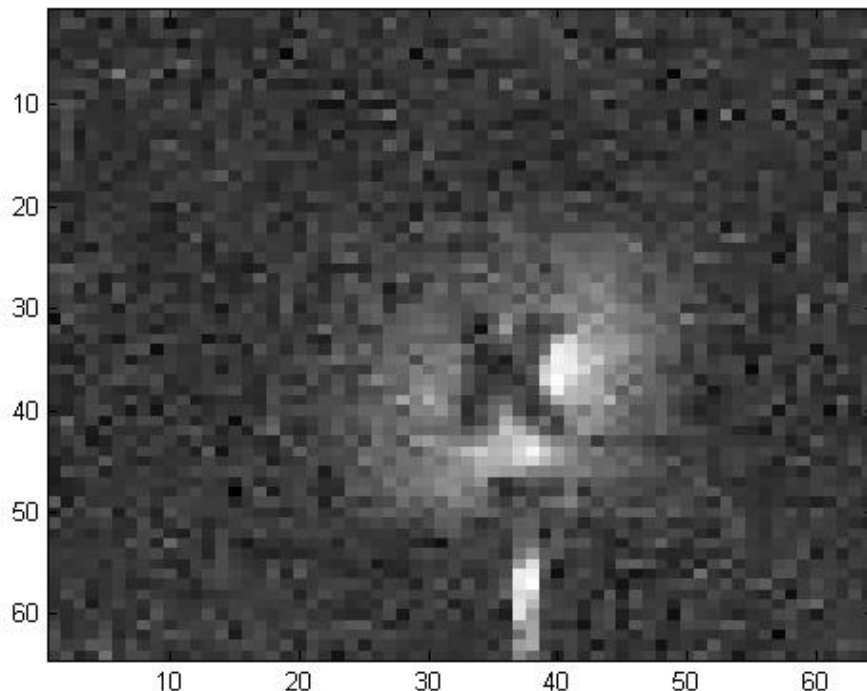


Figure 5.2: 64x64 image, taken using 1600 Walsh patterns

With this project, we have made a start on the process of incorporating CS technology into a practical NIR camera. This type of camera requires only a single photodetector, which means it has the potential to be at least ten times ten times cheaper than current systems on the market. From this project, we have observed that the two main challenges in creating such a camera are as follows:

- Achieving a high enough NIR signal after reflection off a target object, and
- Speeding mirror control to lower image capture time.

Although we mostly concentrated on a projector-based approach during this project, it seems that the restrictive nature of the projector may not make it the best choice for development of this type of camera. Further investigation of the TI Discovery Board alternative would be worthwhile.

To give a broader perspective on what can be done with a good NIR camera, we conclude with a brief overview of potential application areas for a single-pixel NIR camera.

NIR imaging has a wide and expanding array of application areas. These include medical imaging, energy auditing, PCB fault analysis, food quality monitoring, and underdrawing imaging. For medical imaging, NIR tomography, when combined with MRI images, is useful for detecting breast tumors [19]. In the energy auditing field, NIR cameras can determine which parts of a building are hot/cold greedy. This helps architects and construction crews to design and build more eco-friendly structures. In terms of PCB fault analysis, NIR imaging is used to pinpoint hot/cold elements on a chip, to spot current leakage [15]. In

the food quality realm, foods that require high-temperature cooking are candidates for NIR monitoring [6]. In terms of underdrawing imaging, NIR cameras provide access to painter's planning sketches. This allows art collectors to verify the authenticity of works of art that they buy, and gives scholars a chance to examine the old masters' creative processes.

Chicken Nuggets



Figure 5.3: Monitoring heat distribution in chicken nuggets as they cook ensures quality, bacteria-free meat will emerge at the end of a conveyor belt oven [6].

NIR Image of a House



Figure 5.4: Energy audit of a home, showing areas where the house fails to retain heat [7].

Bibliography

- [1] <http://www.maxmax.com/aXRayIRCameras.htm>, October 2007.
- [2] <http://en.wikipedia.org/wiki/Infrared>, October 2007.
- [3] <http://www.dsp.ece.rice.edu/cs/cscamera/>, October 2007.
- [4] http://www.bccrc.ca/images/ci/adlугan_dmd_schematic.jpg, October 2007.
- [5] <http://www.dsp.ece.rice.edu/cs/cscamera/>, October 2007.
- [6] http://atrp.gatech.edu/pt19-1/core_temp_nuggets.jpg, November 2007.
- [7] http://techalive.mtu.edu/meec/module13/images/building_IR.jpg, November 2007.
- [8] Applications overview. <http://www.sensorsinc.com/overview.html>, October 2007.
- [9] Casandra. <http://www.prip.tuwien.ac.at/Research/Casandra/index.htm>, October 2007.
- [10] Cps 200e. http://www.art-innovation.nl/ventura/engine.php?Cmd=seepicture&P_site=316%P_self=450&Random=1203890474, October 2007.
- [11] Grayscale hill. <http://carol.gimp.org/GIMP/howto/desaturate/decompose-gray-RGB.png>, November 2007.
- [12] Psychtoolbox. <http://psychtoolbox.org/>, December 2007.
- [13] R. Baraniuk. Compressive sensing. *IEEE Signal Processing Magazine*, 24, July 2007.
- [14] S. Baronti, A. Casini, F. Lotti, and S. Porcinai. Multispectral imaging system for the mapping of pigments in works of art by use of principal-component analysis. *Applied Optics*, 37(8):1299 – 1309, March 1998.
- [15] F. Beaudoin, G. Imbert, P. Perdu, and C. Trocque. Current leakage fault localization using backside obirch. *Physical and Failure Analysis of Integrated Circuits, 2001. IPFA 2001. Proceedings of the 2001 8th International Symposium on the*, page 1218211;125, 2001.
- [16] D. Bertani, M. Cetica, P. Poggi, G. Puccioni, E. Buzzegoli, D. Kunzelman, and S. Cecchi. A scanning device for infrared reflectography. *Studies in Conservation*, 35(3):113–116, August 1990.
- [17] A. Burmester and F. Bayerer. Towards improved infrared reflectograms. *Studies in Conservation*, 38(3):145–154, August 1993.
- [18] G. Hewlett D. Doherty. 10.4: Phased reset timing for improved digital micromirror device (dmd) brightness. <http://citeseer.ist.psu.edu/243072.html>, 1998.
- [19] H. Dehghani, B.W. Pogue, and K.D. Paulsen. Development of hybrid nir/mri imaging system algorithm: use of a-priori information for tumor detection in the female breast. *Proc. IEEE Int. Symp. on Biomedical Imaging*, page 6578211;60, 2002.

- [20] M. Gargano, N. Ludwig, and G. Poldi. A new methodology for comparing ir reflectographic systems. *Infrared Physics & Technology*, 49:249–253, January 2007.
- [21] Texas Instruments. Dmd discovery 1100: Controller board and starter kit. <http://focus.ti.com/download/dlpdmd/DiscoveryStarterKit.pdf>, 2004.
- [22] A. Lichty. personal communication, October 2007.
- [23] A. Lichty. personal communication, October 2007.
- [24] A. Richards. Near-ir focal-plane arrays improve camera performance. *Compound Semiconductor*, March 2003.
- [25] D. Saunders, N. Atkinson, J. Cupitt, H. Liang, C. Sawyers, and R. Bingham. Siris: a high resolution scanning infrared camera for examining paintings. In R. Salimbeni and L. Pezzati, editors, *Optical Methods for Arts and Archaeology. Edited by Salimbeni, Renzo; Pezzati, Luca. Proceedings of the SPIE, Volume 5857, pp. 205-216 (2005).*, volume 5857 of *Presented at the Society of Photo-Optical Instrumentation Engineers (SPIE) Conference*, pages 205–216, August 2005.
- [26] J. R. J. van Asperen de Boer. Infrared reflectography: a method for the examination of paintings. *Applied Optics*, 7(9):1711–1714, 1968.

Index of Keywords and Terms

Keywords are listed by the section with that keyword (page numbers are in parentheses). Keywords do not necessarily appear in the text of the page. They are merely associated with that section. *Ex.* apples, § 1.1 (1) **Terms** are referenced by the page they appear on. *Ex.* apples, 1

- | | |
|--|--|
| C compressed, § 1(1), § 2(7), § 3(11), § 4(19), § 5(25) | L lab, § 4(19) |
| compressive, § 1(1), § 2(7), § 3(11), § 4(19), § 5(25) | P projector, § 3(11) |
| I imaging, § 1(1), § 3(11), § 4(19), § 5(25) | S sensing, § 2(7)
summary, § 5(25) |

Attributions

Collection: *NIR Single Pixel Camera*

Edited by: J. Ryan Stinnett, Jennifer Gillenwater

URL: <http://cnx.org/content/col10525/1.1/>

License: <http://creativecommons.org/licenses/by/2.0/>

Module: "Project Introduction"

By: J. Ryan Stinnett, Jennifer Gillenwater

URL: <http://cnx.org/content/m16124/1.1/>

Pages: 1-5

Copyright: J. Ryan Stinnett, Jennifer Gillenwater

License: <http://creativecommons.org/licenses/by/2.0/>

Module: "Compressive Imaging"

By: J. Ryan Stinnett, Jennifer Gillenwater

URL: <http://cnx.org/content/m16125/1.1/>

Pages: 7-10

Copyright: J. Ryan Stinnett, Jennifer Gillenwater

License: <http://creativecommons.org/licenses/by/2.0/>

Module: "Projector Setup and Issues"

By: J. Ryan Stinnett, Jennifer Gillenwater

URL: <http://cnx.org/content/m16126/1.1/>

Pages: 11-18

Copyright: J. Ryan Stinnett, Jennifer Gillenwater

License: <http://creativecommons.org/licenses/by/2.0/>

Module: "DMD Development Kit Setup and Issues"

By: J. Ryan Stinnett, Jennifer Gillenwater

URL: <http://cnx.org/content/m16127/1.1/>

Pages: 19-24

Copyright: J. Ryan Stinnett, Jennifer Gillenwater

License: <http://creativecommons.org/licenses/by/2.0/>

Module: "Project Summary"

By: J. Ryan Stinnett, Jennifer Gillenwater

URL: <http://cnx.org/content/m16128/1.1/>

Pages: 25-29

Copyright: J. Ryan Stinnett, Jennifer Gillenwater

License: <http://creativecommons.org/licenses/by/2.0/>

NIR Single Pixel Camera

Describes our work on building an NIR single pixel camera for our senior design project.

About Connexions

Since 1999, Connexions has been pioneering a global system where anyone can create course materials and make them fully accessible and easily reusable free of charge. We are a Web-based authoring, teaching and learning environment open to anyone interested in education, including students, teachers, professors and lifelong learners. We connect ideas and facilitate educational communities.

Connexions's modular, interactive courses are in use worldwide by universities, community colleges, K-12 schools, distance learners, and lifelong learners. Connexions materials are in many languages, including English, Spanish, Chinese, Japanese, Italian, Vietnamese, French, Portuguese, and Thai. Connexions is part of an exciting new information distribution system that allows for **Print on Demand Books**. Connexions has partnered with innovative on-demand publisher QOOP to accelerate the delivery of printed course materials and textbooks into classrooms worldwide at lower prices than traditional academic publishers.